

# Research on Laser Welding of Mg-Rare Earth Alloy Mg-3Nd-0.2Zn-0.4Zr

Jun Dai, Jian Huang, and Yixiong Wu

(Submitted October 30, 2010)

The welding process of Mg-rare earth alloy Mg-3Nd-0.2Zn-0.4Zr (NZ30K) was studied using 15 kW high-power CO<sub>2</sub> laser, the microstructure and performance of the typical welded joints had been analyzed and tested. There is no softening zone according to the microhardness test of the welded joint. The microstructure of the fusion zone consists of  $\alpha$ -Mg-phase and  $\beta$ -phase (Mg<sub>12</sub>Nd). The results show that Mg-rare earth alloy NZ30K can be well joined with the high power laser and the welded joint has good performance.

**Keywords** high-power CO<sub>2</sub> laser, laser welding, Mg-rare earth alloy, NZ30K

## 1. Introduction

Today, magnesium alloy is well known as the twenty-first century green project material because of environment-friendly, lightweight, energy-saving, and satisfying the requirement of sustainable development. Hence, the magnesium alloy is used more and more in automotive, electronics, aerospace, and other fields (Ref 1, 2). As the unique electronic structure of rare earth elements and performance, in recent years the rare earth elements have been widely used in alloy materials. Since the excellent properties, many researchers have been focus on the Mg-rare earth alloy. More and more Mg-rare earth alloy has been developed and applied (Ref 3-5).

A new Mg-rare earth alloy NZ30K alloyed with the rare earth element neodymium (Nd) has been developed, researchers have investigated the microstructure and mechanical properties as well as the corrosion behaviors of NZ30K alloy (Ref 6, 7). It can be used as components in transportation system, parts in the car, and bracket of car engines (Ref 8). However, it is difficult to obtain high-quality welding joints by conventional welding methods. High-power CO<sub>2</sub> laser can reduce the magnesium alloy welding defects because of its unique advantages. There are plenty of researches on laser welding of conventional magnesium alloys (Ref 9-11). However, the laser welding research on thick magnesium alloy plate and Mg-rare earth alloy is quite less.

In this article, the microstructure and performance of the welded joints of thick Mg-rare earth alloy using high-power CO<sub>2</sub> laser were investigated.

Jun Dai, Jian Huang, and Yixiong Wu, Shanghai Key Laboratory of Materials Laser Processing and Modification, School of Materials Science and Engineering, Shanghai Jiao Tong University, Shanghai 200240, P.R. China. Contact e-mails: 83djun@sjtu.edu.cn and jhuang@sjtu.edu.cn.

## 2. Experimental Materials and Methods

The experimental material is the hot-rolled Mg-rare earth alloy NZ30K, which is alloyed by the rare earth element Nd and the elements Zinc (Zn) and Zirconium (Zr). Its chemical composition is listed in Table 1.

The microstructure of the base metal (BM) is shown in Fig. 1. A hot-rolled strip organization without the obvious grain boundary could be observed.

The size of test specimens is 150 \* 50 \* 9.5 mm. A maximum output power of 15 kW CO<sub>2</sub> Laser source (TRUMPF TLF15000T) was used. The diameter of the laser beam focus is 0.8 mm. The pure helium was used as side-blown gas and the back side of specimens was protected by pure Argon.

Before welding, the surface oxide film of the specimens was removed using a steel brush and then cleaned by acetone. The laser butt welding parameters are listed in Table 2. The microstructure of the typical welds was observed by JSM-6460 Scanning Electron Microscope. The hardness of welded joints was tested using a digital Vickers hardness tester and the tensile properties were tested by a Zwick Z020 E-stretching machine.

## 3. Results

### 3.1 Cross section of Weld Bead

The cross section of the welding sample is shown in Fig. 2. The welding sample is full penetration and no macroscopic defects in the welded joint.

### 3.2 Microstructure of Welded Joint

Figure 3 describes the microstructure of the welded joint. As seen from Fig. 3, the right area is the fusion zone (FZ) that consists of numerous small equiaxed grains. The left area is the heat affected zone (HAZ) consisting of big grains with evident grain boundary. The HAZ area has slight hot-rolled strip organization.

Figure 4 displays the microstructure of the FZ. As NZ30K alloy contains Zr element that acts as the grain refiner during the solidification, the chances of nonspontaneous nucleation would be increased, which could prompts the formation of equiaxed grains in the FZ. Also, the energy of high-power CO<sub>2</sub>

**Table 1 Chemical compositions of the NZ30K (wt.%)**

Compositions	Nd	Zn	Zr	Fe	Ni	Mg
Content	2.5-3.5	0.2-0.4	0.3-0.5	<0.002	<0.002	Balance

**Table 2 Typical welding parameters**

Laser power P, kW	Welding speed v, m/min	Focal position Fp, mm	He gas flow Q1, L/min	Ar gas flow Q2, L/min
7	2.8	-2	25	20

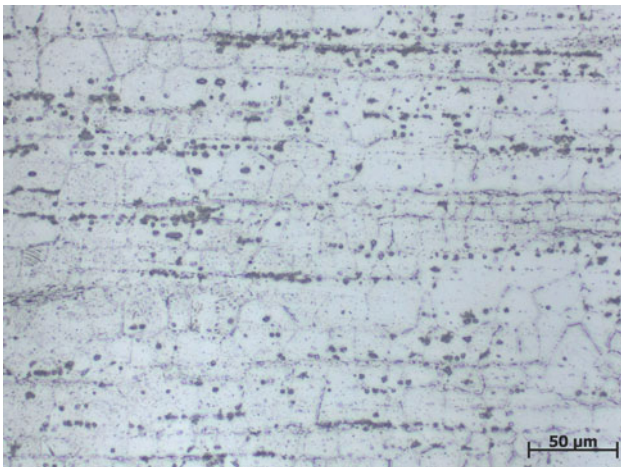


**Fig. 1** Microstructure of the base metal

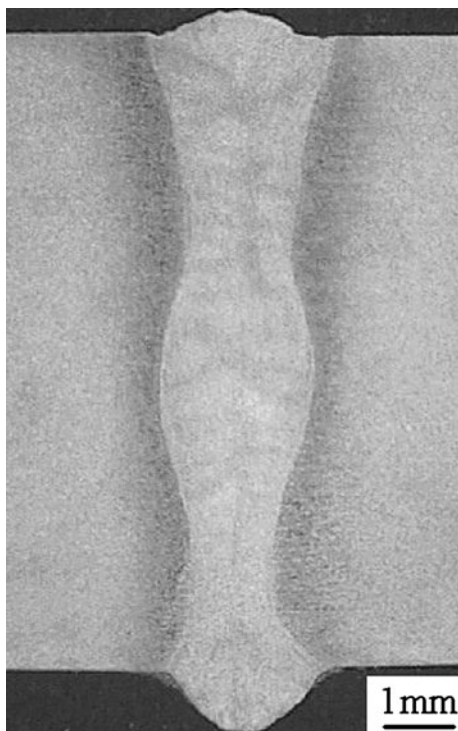


**Fig. 2** Cross section of the welded joint

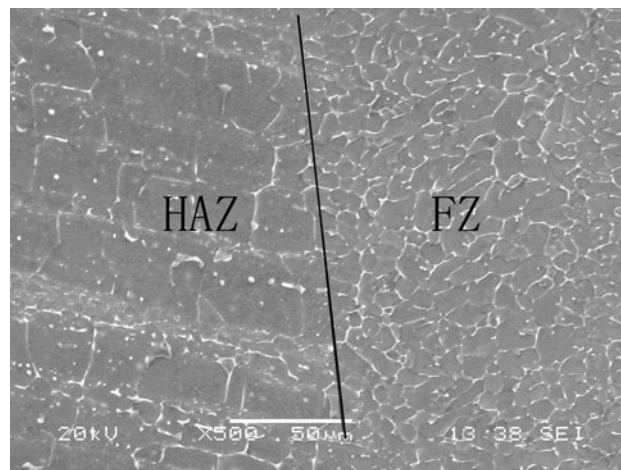


**Fig. 3** Microstructure of the welded joint

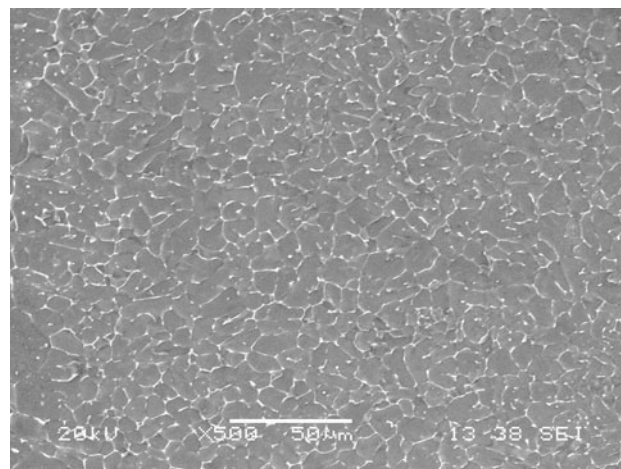


**Fig. 4** Microstructure of the fusion zone

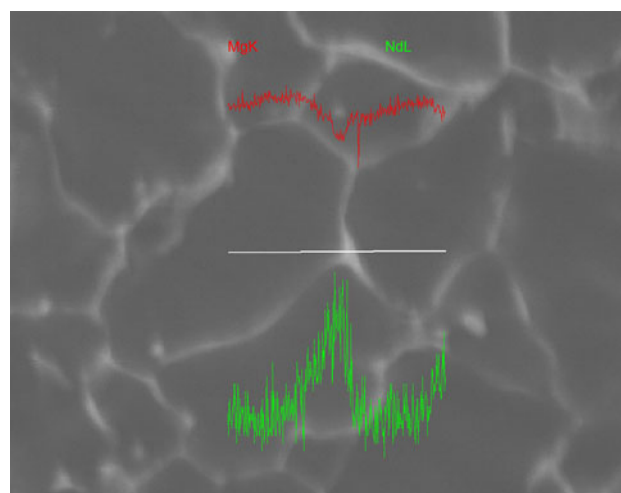


**Fig. 5** Mg(K) and Nd(L) distribution by EDX line-scan

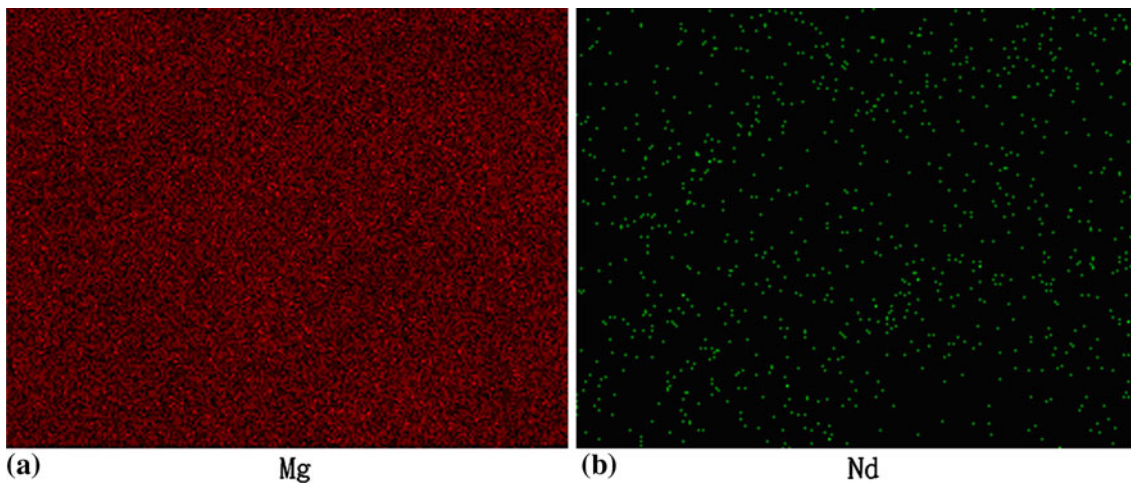


Fig. 6 Mg(K) and Nd(L) distribution by EDX map-scan

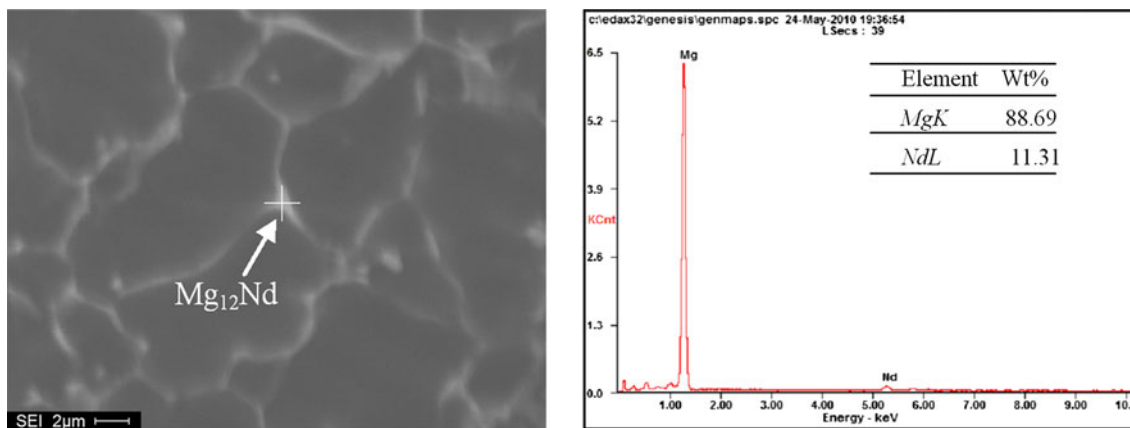


Fig. 7 EDX results of grain boundary

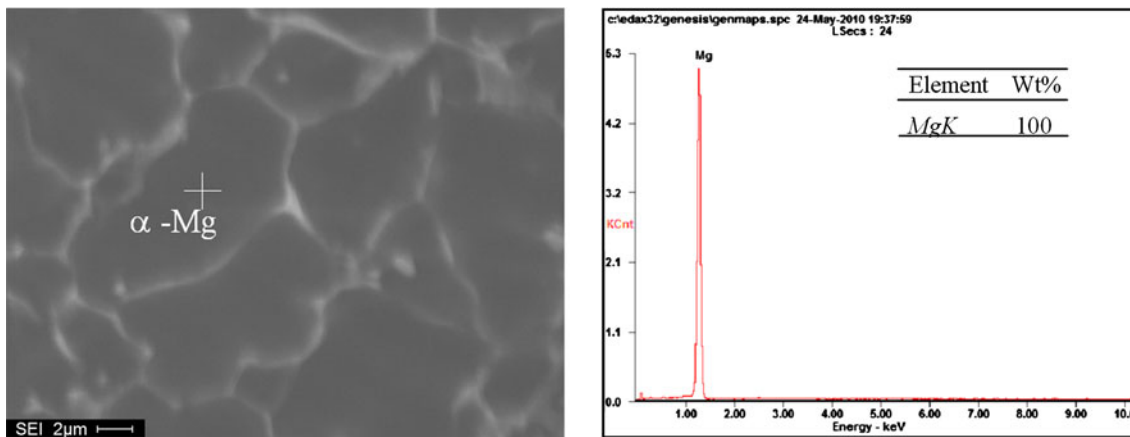


Fig. 8 EDX results of grain interior

laser beam is quite focused, fast cooling rate, and crystallization rate can also contribute to refine the size of the grain in the FZ.

### 3.3 The Element Distribution Analysis

To observe the element distribution of weld metal, the main elements, such as Mg, Nd were analyzed using

energy-dispersive x-ray (EDX) spectrometry. Results are shown in Fig. 5 and 6. Nd presented enrichment at the crystal boundary.

Figures 7 and 8 shows the results of phase analyses in the grain interior and grain boundary by the EDX. The FZ mainly consists of  $\alpha$ -Mg-phase as base and  $\beta$ -phase ( $Mg_{12}Nd$ ) which distributed along the grain boundary.

### 3.4 Mechanical Properties of the Welded Joint

**3.4.1 Tensile Strength of the Welded Joint.** The results of the tensile strength are listed in Table 3. Tensile specimens were broken in the BM region. It can be seen from the Table 3 that the tensile strength of welded joint is almost the same as that of base material, this is due to the grain refinement in FZ.

**3.4.2 Microhardness of the welded joint.** Figures 9 and 10 display the Vickers microhardness of the welded joint. The microhardness distribution shows that the hardness across the

**Table 3 Tensile strength of welded joint and BM**

Sample	Rp 0.2, N/mm <sup>2</sup>	Rm, N/mm <sup>2</sup>	Agt, %
Welded joint	108.60	198.56	6.68
BM	104.4	195.2	5.02

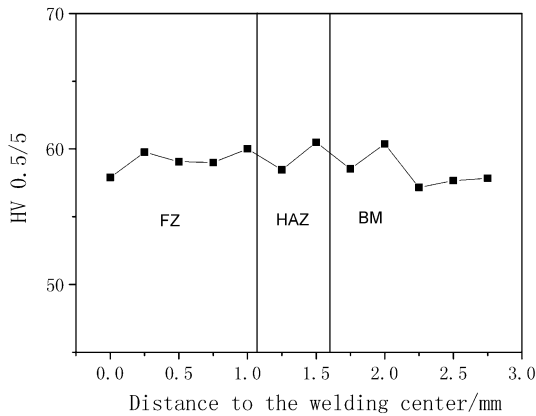


**Fig. 9** Microhardness distribution across the welded joint

welded joint is almost the same. There is no obvious softening zone in welded joint. The microhardness along the weld depth has almost no change.

## 4. Discussion

The phase diagram of Mg-Nd is shown in Fig. 11. When the high power laser focused to the surface of the alloy NZ30K, the temperature of the alloy became higher, then turned to liquid in a very short time. After the laser went on, the temperature of the alloy became down. When the liquid alloy cooled to 650 °C, it began to generate  $\alpha$ -Mg solidification. When the temperature was about 548 °C, the eutectic solidification reaction occurred. Since a large number of  $\alpha$ -Mg had already frozen, the  $Mg_{12}Nd$

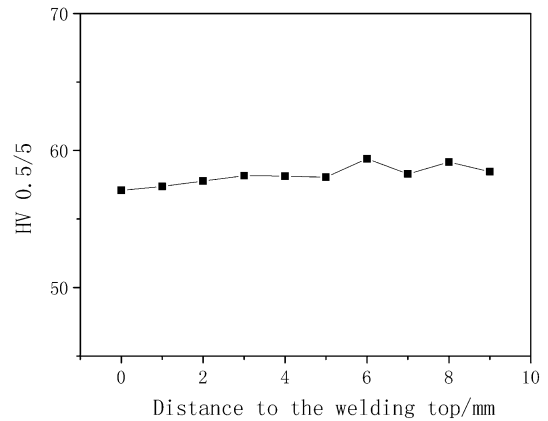


**Fig. 10** Microhardness of the weld bead in depth direction

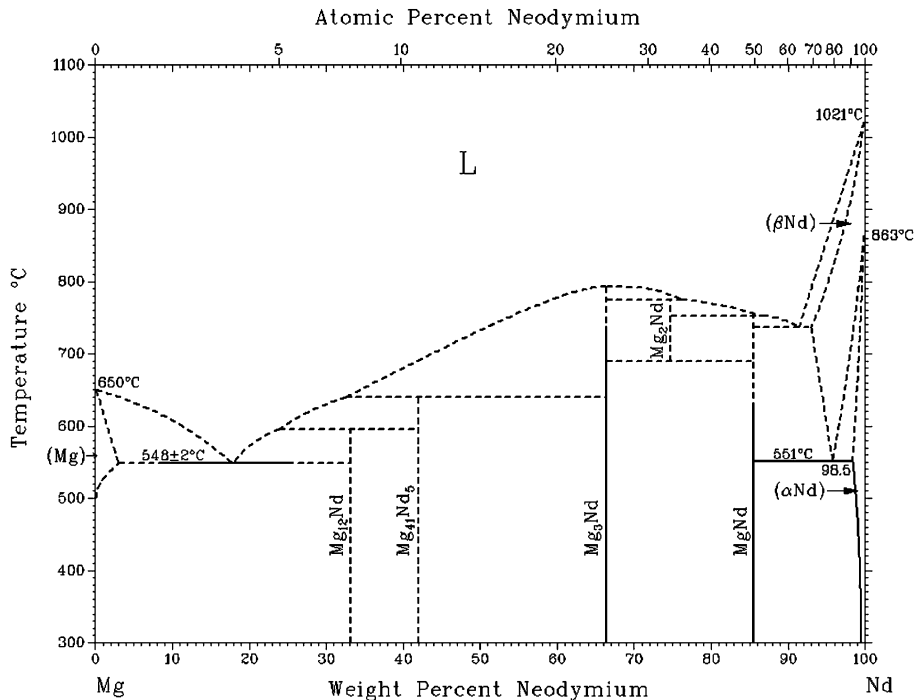


**Fig. 11** Phase diagram of Mg-Nd



had to distribute along the grain boundary as shown in the Fig. 7. Because of the good thermal stability of  $Mg_{12}Nd$ , it could play on the grain growth impediment to further refine the grain.

The main problems about welding of Mg alloy by conventional processing methods are the appearance of excessive porosity, oxide inclusions, the softening HAZ, and loss of alloying elements (Ref 2). However, the welded joint of high-power  $CO_2$  laser welding of NZ30K alloy can be deserved good quality with appropriate process.

## 5. Conclusions

From the investigation, the results and conclusions are summarized as follows:

- (i) The 9.5 mm thickness Mg-rare earth alloy NZ30K can be well welded by the high-power  $CO_2$  laser. The welded joint has good performance.
- (ii) The FZ mainly consists of  $\alpha$ -Mg-phase as base and  $\beta$ -phase ( $Mg_{12}Nd$ ) which distributes along the grain boundary.

## Acknowledgments

The authors would like to thank Jie Dong and Fenghua Wang from National Engineering Research Center of Light Alloys Net Forming for providing the experimental materials.

## References

1. C. Shi, H. Li, D. Wang, and Y. Li, A Proposal on Accelerating Development of Metallic Magnesium Industry in China, *Mater. Rev.*, 2001, **4**, p 5–6
2. X. Cao, M. Jahazi, J.P. Immariageon, and W. Wallace, A Review of Laser Welding Techniques for Magnesium Alloys, *J. Mater. Process. Technol.*, 2006, **171**, p 188–204
3. T. Honma, Chemistry of Nanoscale Precipitates in Mg-2.1 Gd-0.6 Y-0.2 Zr (at.%) Alloy Investigated by the Atom Probe Technique, *Mater. Sci. Eng. A*, 2005, **395**, p 301–306
4. T.L. Chia, The Effect of Alloy Composition on the Microstructure and Tensile Properties of Binary Mg-Rare Earth Alloys, *Intermetallics*, 2009, **17**(7), p 481–490
5. T.J. Pike and B. Noble, The Formation and Structure of Precipitates in a Dilute Magnesium-Neodymium alloy, *J. Less Common Met.*, 1973, **30**(1), p 63–74
6. F. Penghuai, Effects of Heat Treatments on the Microstructures and Mechanical Properties of Mg-3Nd-0.2 Zn-0.4 Zr (wt%) Alloy, *Mater. Sci. Eng. A*, 2008, **486**, p 183–192
7. J.W. Chang, The Effects of Heat Treatment and Zirconium on the Corrosion Behaviour of Mg-3Nd-0.2 Zn-0.4 Zr (wt%) Alloy, *Corros. Sci.*, 2007, **49**(6), p 2612–2627
8. X. Zheng, Formability, Mechanical and Corrosive Properties of Mg-Nd-Zn-Zr Magnesium Alloy Seamless Tubes, *Mater. Des.*, 2010, **31**(3), p 1417–1422
9. M. Marya and G.R. Edwards, Factors Controlling the Magnesium Weld Morphology in Deep Penetration Welding by a  $CO_2$  Laser, *J. Mater. Eng. Perform.*, 2001, **10**(4), p 435–443
10. M. Dhahri, J.E. Masse, J.F. Mathieu, and G. Barreau,  $CO_2$  Laser Welding of Magnesium Alloys, *Proceedings of the SPIE: High-Power Lasers in Manufacturing*, 2000, p 725–732
11. B.L. Mordike and T. Ebert, Magnesium: Properties-Applications-Potential, *Mater. Sci. Eng. A*, 2001, **302**, p 37–45